A theoretical analysis of zero-field splitting of Mn^{2+} in sodium nitrite

1996 J. Phys.: Condens. Matter 8 6759

(http://iopscience.iop.org/0953-8984/8/36/026)

J. Phys.: Condens. Matter **8** (1996) 6759–6767. Printed in the UK

A theoretical analysis of zero-field splitting of Mn^{2+} in sodium nitrite

Kee Tae Han and Jongmin Kim

Department of Electronics and Optics, Agency for Defense Development, Taejeon 305-600, Korea

Received 23 January 1996, in final form 30 April 1996

Abstract. The point-charge electrostatic model and the superposition model have been used to investigate the substitution of Mn^{2+} for either the Na^+ or the N^{3+} site in sodium nitrite ($NaNO_2$). The zero-field splitting (ZFS) parameters D and E at both sites calculated by these models are compared with the experimental values D_{exp} and E_{exp}, respectively, for Mn^{2+} electron spin resonance. Both models give rise to the same results. The theoretical ZFS parameters D_{Na} and E_{Na}, for Mn^{2+} at Na^+ sites turn out to be more similar to the experimental values than are the parameters D_N and E_N, respectively, at N^{3+}. This result means that the Mn^{2+} impurity should substitute for the Na^+ ion in an $NaNO_2$ crystal, which is well supported by a comparison of the chemical properties such as the ionic radii of Mn^{2+}, Na^+ and N^{3+} and the bond lengths of Mn^{2+}–O^{2-}, Na^+–O^{2-} and N^{3+}–O^{2-} and by the consideration of the covalency of the NO_2^- radical.

1. Introduction

Many studies of the ^{23}Na nuclear magnetic resonance (NMR) and ^{14}N nuclear quadrupole resonance in $NaNO_2$ have been made to investigate the change in the charge distribution around the resonant nuclei due to external effects (Yagi and Tasuzaki 1973, Serishev *et al* 1974, Ambroseti *et al* 1977, Han *et al* 1990, Han and Choh 1992, 1993), whereas few electron spin resonance (ESR) studies have been made to enquire into the radiation effect in a γ-ray-irradiated $NaNO_2$ crystal (Takeno and Gesi 1964, Luz *et al* 1969) and the temperature effect on D of Mn^{2+} in Mn-doped $NaNO_2$ (Jain *et al* 1978, Jain and Upreti 1978). Incidentally, the temperature dependence of the experimental D reported by Jain *et al* was analysed in terms of the ferroelectric soft phonon effect without mentioning the occupation site of Mn^{2+}. Since the temperature dependence of D closely relies on its occupation site, it is necessary to investigate the occupation site of Mn^{2+}. However, both Na^+ and N^{3+} sites have the same point symmetry (C_{2v}) so that the probable site of Mn^{2+} cannot be estimated directly from the rotation pattern of ESR signals.

Therefore, the zero-field splitting (ZFS) parameters for the Mn^{2+} ion, assuming that it is located at either the Na^+ or the N^{3+} site, have been calculated using the superposition model (SPM) and the point-charge electrostatic model (PCM). These models have been widely used as quite reliable for determining the probable site of a dopant (see, e.g., Yu (1990) and Yeom *et al* (1993, 1996). The theoretical results obtained with these models are compared to the experimental data, and thus the preferred site of Mn^{2+} in an $NaNO_2$ crystal is considered. In addition, the ionic radii of Mn^{2+}, Na^+ and N^{3+} as well as the bond lengths of Mn–O, Na–O and N–O are compared with one another to check the possibility

0953-8984/96/366759+09$19.50

of the results determined by the two models, and the covalency of the NO_2^- radical is also considered seriously.

2. Crystal structure of $NaNO_2$

$NaNO_2$ is a body-centred orthorhombic compound with the space group C_{2v}^{20} ($Im2m$) in the ferroelecric phase ($T_c < 436.5$ K), and with the space group D_{2h}^{25} ($Immm$) in the paraelectric phase. This material is an order–disorder-type ferroelectrics (Nomura 1961). Its ferroelectricity comes from the relative difference between the Na^+–NO_2 distances along the $+b$ and along the $-b$ axis, accompanied by ordering of the NO_2^- dipoles. The unit cell of $NaNO_2$ has two molecules and the cell dimensions are $a = 3.560$ Å, $b = 5.560$ Å and $c = 5.384$ Å at room temperature (RT). The other structural data at RT (Kay and Frazer 1961, Kay 1972) are shown in table 1, and the coordinates of O^{2-} ions from the Na^+ or N^{3+} ions are listed in table 2.

Table 1. Crystal structure data for an orthorhombic unit cell of $NaNO_2$ having two molecules (RT; $a = 3.560$ Å, $b = 5.560$ Å and $c = 5.384$ Å; $t = 0.5853 \pm 0.0010$, $w = 0.1200 \pm 0.0007$, $u = 0.0000 \pm 0.0006$ and $v = 0.1941 \pm 0.0006$).

	Molecule 1			Molecule 2		
Atoms	a	b	c	a	b	c
Na	0	$0+t$	0	$\frac{1}{2}$	$\frac{1}{2}+t$	$\frac{1}{2}$
N	0	$0+w$	0	$\frac{1}{2}$	$\frac{1}{2}+w$	$\frac{1}{2}$
O	0	$0+u$	$0+v$	$\frac{1}{2}$	$\frac{1}{2}+u$	$\frac{1}{2}+v$
O	0	$0+u$	$0-v$	$\frac{1}{2}$	$\frac{1}{2}+u$	$\frac{1}{2}-v$

Table 2. The spherical coordinates of O^{2-} ions from the Na^+ and N^{3+} sites at room temperature.

	First-nearest neighbours			Second-nearest neighbours		
	R (Å)	θ (deg)	ϕ (deg)	R (Å)	θ (deg)	ϕ (deg)
Na^+	2.47	102	42.8	2.52	24.4	90
	2.47	102	137.2	2.52	24.4	270
	2.47	102	222.8			
	2.47	102	317.2			
N^{3+}	1.23	122.2	90	3.22	48.9	42.8
	1.23	122.2	270	3.22	48.9	137.2
				3.22	48.9	222.8
				3.22	48.9	317.2

For the Na^+ site, there are four first-nearest-neighbour oxygen ions and two second-nearest neighbours in the ferroelectric phase (see table 2). The distances (2.47 Å) of the Na atom to the first-nearest oxygen neighbours are very similar to those (2.52 Å) of the second-nearest neighbours. For the N^{3+} site, however, there are two first-nearest oxygen ligands and four next-nearest neighbours. The distances (1.23 Å) of the N atom to the first-nearest neighbours are even shorter than those (3.22 Å) of the next nearest neighbours.

3. Theoretical background

The usual spin Hamiltonian describing the Mn^{2+} ESR results for $NaNO_2$ is given by

$$H = \beta \boldsymbol{B}\cdot\mathbf{g}\cdot\boldsymbol{S} + (B_2^0O_2^0 + B_2^2O_2^2 + B_4^0O_4^0 + B_4^2O_4^2 + B_4^4O_4^4) + \boldsymbol{S}\cdot\mathbf{A}\cdot\boldsymbol{I} \tag{1}$$

where β is the Bohr magneton, $\boldsymbol{B}$ the external magnetic field, $\mathbf{g}$ the spectroscopic splitting tensor, $\boldsymbol{S}$ the effective electronic spin vector, $\mathbf{A}$ the hyperfine tensor and $\boldsymbol{I}$ the nuclear spin vector. $B_2^0(=D/3)$ and $B_2^2(=E/3)$ in the parentheses are the second-order axial and the rhombic ZFS parameters, respectively. The terms on the right-hand side of equation (1) stand for the Zeeman interaction, the fine structure and the hyperfine interaction, respectively.

The energy levels of the first two terms in equation (1) can be obtained by numerically diagonalizing the 6×6 matrix of the $|S, S_z\rangle$ states with $S=\frac{5}{2}$ (Mn^{2+} ion) in terms of the Jacobi rotation method. The ESR parameters can be determined from the best fit satisfying simultaneously the resonance field data measured on the crystallographic *a*–*b*-, *b*–*c*- and *c*–*a*-planes, when all allowed transitions are considered. The experimental ESR parameters D_{exp} and E_{exp} at RT were taken from the previous report (Jain *et al* 1978): $D_{exp}=0.0464$ and $E_{exp}=-0.0144$ cm^{-1}. However, the preferred site of Mn^{2+} cannot be seen directly from the rotation pattern of ESR signals because both Na^+ and N^{3+} sites have the same point symmetry.

The effect of the spin–orbit interaction is dealt with as a perturbation to the free-ion Hamiltonian. However, the spin–spin interaction is neglected owing to its small contribution compared with the spin–orbit interaction (Sharma *et al* 1966, Sharma 1967, 1968). In rhombic symmetry, the ZFS parameters D and E are given by (Yu and Zhao 1987, 1988)

$$\begin{aligned} D^{(4)}(\mathrm{SO}) &= (3\zeta^2/70P^2D)(-B_{20}^2 - 21\zeta B_{20} + 2B_{22}^2) \\ &\quad +(\zeta^2/63P^2G)(-5B_{40}^2 - 4B_{42}^2 + 14B_{44}^2) \\ E^{(4)}(\mathrm{SO}) &= (3\zeta^2/70P^2D)(2B_{20} - 21\zeta)B_{22} + (\zeta^2/63P^2G)(3\sqrt{10}B_{40} + 2\sqrt{7}B_{44})B_{42} \end{aligned} \tag{2}$$

where $P=7B+7C$, $G=10G+5C$ and $D=17B+5C$. B and C are the Racah parameters describing the electron–electron repulsion. Considering the covalency effect, the parameters B and C are given by (Zhao and Zhang 1983, Zhao *et al* 1987)

$$B = N^4B_0 \qquad C = N^4C_0 \tag{3}$$

where N is the average covalency parameter, and $B_0(C_0)$ the value in the free state. Also, ζ is the spin–orbit coupling, which could be reduced to the product of N^2 and ζ_0 (the value in the free state) in a crystal. Meanwhile, the first-, second-, third- and fifth-order perturbations of D and E are zero, and the sixth-order term is small enough to be negligible. Thus only the fourth-order term is considered here.

The crystal-field parameters B_{kq} in equation (2) are closely related to the crystal structure of $NaNO_2$ and are calculated using the following models with the structure data in table 2.

3.1. Point-charge model

Following the PCM, the crystal-field parameters are given by

$$\begin{aligned} B_{kq} &= (-1)^q \sum_i eq_i\langle r^k\rangle \frac{C_q^k(\theta_i,\phi_i)}{R_i^{k+1}} \\ C_q^k &= \sqrt{4\pi/(2k+1)}\,Y_q^k \end{aligned} \tag{4}$$

where R_i, θ_i and ϕ_i are the spherical coordinates of the ith ligand. q_i is the equivalent charge of the ith ligand and Y_q^k are the spherical harmonics (Yu and Zhao 1987, 1988). The expectation value of $\langle r^k \rangle$ for the d^n ion in a crystal is given by

$$\langle r^k \rangle = N^2 \langle r^k \rangle_0 \tag{5}$$

where $\langle r^k \rangle_0$ is the value of the free atom, and N the average covalency parameter.

3.2. Superposition model

As an empirical model, the SPM has been shown to be quite successful in explaining the crystal-field splitting of $4f^n$ and $3d^n$ ions (Newman *et al* 1978, Shen and Zhao 1984). This model expresses the crystal-field parameters as follows (Yu and Zhao 1987, 1988):

$$B_{kq} = \sum_i \overline{A_k}(R_i) K_{kq}(\theta_i, \phi_i) \tag{6}$$

where the coordination factor $K_{kq}(\theta_i, \phi_i)$ is an explicit function of the angular position of the ith ligand ion, and the intrinsic parameter $A_k(R_0)$ is given by

$$\overline{A_k}(R_i) = \overline{A_k}(R_0)(R_0/R_i)^{tk} \tag{7}$$

where R_i is the distance between the d^n ion and the O^{2-} ion, and $A_k(R_0)$ is the intrinsic parameter of the reference crystal, t_k is the power-law exponent.

4. Analysis and discussion

As both Na^+ and N^{3+} ions have the same symmetry (twofold coordination), it cannot be stated directly from the rotation pattern of ESR signals which is effectively occupied by the Mn^{2+} ion. In order to elucidate this, we calculate directly the spin-Hamiltonian parameters using on one hand the PCM and on the other hand the SPM. The crystal-field parameters B_{2q} and B_{4q} are proportional to R_i^{-3} and R_i^{-5}, respectively, in the PCM, and B_{2q} and B_{4q} are proportional to R_i^{-3} and R_i^{-7}, respectively, in the SPM. Moreover, the expression for D and E from equation (2) contains B_{kq}^2 terms. For these reasons, the oxygen ions near to the Na (or N) atom effectively contributes to D and E. For the Na^+ site, the bond lengths (2.47 Å) of Na–O for the first-nearest oxygen ions are very similar to those (2.52 Å) for the second-nearest neighbours; thus even the second-nearest oxygen ions are considered in the calculation. For the N^{3+} site, only the first-nearest neighbours are considered because the bond lengths of N–O for the first-nearest oxygen ions are far shorter than those (3.22 Å) for the second-nearest neighbours (see table 2).

The following values for the free Mn^{2+} ion, obtained from the two Slater-type d orbits, are used:

$$B_0 = 911 \text{ cm}^{-1} \qquad C_0 = 3273 \text{ cm}^{-1} \qquad \zeta_0 = 336.6 \text{ cm}^{-1} \qquad \text{(Zhao } \textit{et al} \text{ 1987)} \tag{8}$$

$$\langle r^2 \rangle_0 = 2.7755 \text{ au} \qquad \langle r^4 \rangle_0 = 23.2594 \text{ au} \qquad \text{(Sharma 1968).} \tag{9}$$

The values of N ($0 < N < 1$; $N = 1$ for the pure ionic bond) were taken from the values of manganese–oxygen bonds in two other crystals ($N = 0.942$ for $MnCO_3$, and $N = 0.956$ for $CaSiO_3$:Mn) (Curie *et al* 1974).

4.1. Point-charge model

The non-zero crystal-field parameters derived from equation (4) are expressed as follows:

$$
\begin{aligned}
B_{20} &= \tfrac{1}{2}e\langle r^2\rangle \sum_i \frac{q_i(3\cos^2\theta_i - 1)}{R_i^3} \\
B_{22} &= (\tfrac{3}{8})^{1/2}e\langle r^2\rangle \sum_i \frac{q_i \sin^2\theta_i \cos(2\phi_i)}{R_i^3} \\
B_{40} &= \tfrac{1}{8}e\langle r^4\rangle \sum_i \frac{q_i(35\cos^4\theta_i - 30\cos^2\theta_i + 3)}{R_i^5} \\
B_{42} &= (\tfrac{5}{32})^{1/2}e\langle r^4\rangle \sum_i \frac{q_i \sin^2\theta_i(7\cos^2\theta_i - 1)\cos(2\phi_i)}{R_i^5} \\
B_{44} &= (\tfrac{35}{128})^{1/2}e\langle r^4\rangle \sum_i \frac{q_i \sin^4\theta_i \cos(4\phi_i)}{R_i^5}.
\end{aligned}
\tag{10}
$$

The parameters B_{kq} in the above equations can be calculated by considering the position of O^{2-} ions from the Na^+ and N^{3+} sites in the $NaNO_2$ unit cell (table 2). In this calculation, we used $q_i = 1.07e$ (Kanashiro *et al* 1985), which was determined from the NMR experiment. The ZFS parameters D_{Na}^{PCM} and E_{Na}^{PCM} for Mn^{2+} at Na^+ sites and the ZFS parameters D_N^{PCM} and E_N^{PCM} at N^{3+} sites calculated by the PCM are shown in table 3, where the experimental ZFS parameters are also listed for comparison. As shown in this table, the order of magnitude of D_{exp} (E_{exp}) is more similar to that of D_{Na}^{PCM} (E_{Na}^{PCM}) than to that of D_N^{PCM} (E_N^{PCM}), and the sign of E_{exp} is in agreement with that of E_{Na}^{PCM} and is opposite to that of E_N^{PCM}. This result indicates that Mn^{2+} ion should replace the Na^+ site.

Table 3. Comparison of the ZFS parameters calculated by the point-charge model for Mn^{2+} at Na^+ and N^{3+} ions in $NaNO_2$ with the experimental data.

	Theoretical				
	Na site		N site		
ZFS parameters	$N = 0.942$	$N = 0.956$	$N = 0.942$	$N = 0.956$	Experimental (Jain *et al* 1978)
D (10^{-4} cm^{-1})	295	263	15 113	14 144	464
E (10^{-4} cm^{-1})	−13	−11	17 202	16 037	−144
E/D	<0	<0	>0	>0	<0

Meanwhile, when the Mn^{2+} ion substitutes for the Na^+ site, charge compensation appears. This problem may cause one Mn^{2+} ion to couple with two adjacent NO_2^- radicals, resulting in the formation of $Mn(NO_2)_2$ and an Na^+ vacancy near to this molecule. Here, we can expect the quite reasonable situation that the structural arrangement of O^{2-} nearest to the Mn^{2+} ion still remains without any change due to the compensating charge. In this situation, the effect of nearby charge compensation can be neglected because the nearest oxygen ions more effectively contribute to the ZFS parameters. Thus, it is reasonable to calculate the ZFS parameters for Mn^{2+} at Na^+ sites from equations (4) and (6).

4.2. Superposition model

According to this model, the crystal-field parameters B_{kq} obtained from equations (6) and (7) can be expressed by

$$\begin{aligned}
B_{20} &= \overline{A_2}(R_0)\sum_i \left(\frac{R_0}{R_i}\right)^3 (3\cos^2\theta_i - 1) \\
B_{22} &= (\tfrac{6}{4})^{1/2}\overline{A_2}(R_0)\sum_i \left(\frac{R_0}{R_i}\right)^3 \sin^2\theta_i \cos(2\phi_i) \\
B_{40} &= \overline{A_4}(R_0)\sum_i \left(\frac{R_0}{R_i}\right)^7 (35\cos^4\theta_i - 30\cos^2\theta_i + 3) \\
B_{42} &= (10)^{1/2}\overline{A_4}(R_0)\sum_i \left(\frac{R_0}{R_i}\right)^7 \sin^2\theta_i(7\cos^2\theta_i - 1)\cos(2\phi_i) \\
B_{44} &= (\tfrac{35}{2})^{1/2}\overline{A_4}(R_0)\sum_i \left(\frac{R_0}{R_i}\right)^7 \sin^4\theta_i \cos(4\phi_i).
\end{aligned} \tag{11}$$

The parameter $\overline{A_k}(R_0)$ can be obtained from the crystal-field splitting. As usual, the crystal-field splittings of an ion within the same bond are similar for different crystals. Likewise, the intrinsic parameters $\overline{A_2}$ and $\overline{A_4}$ of the bond in different crystals are similar to one another (Yeom *et al* 1996). For the Mn^{2+} ion in an $NaNO_2$ crystal, the parameters $\overline{A_2}$ and $\overline{A_4}$ have not been determined yet; thus we obtain them by inserting the values $N = 0.942$ or $N = 0.956$ and $R_0 = 2.1$ Å into the following theoretical equations (Shen and Zhao 1984):

$$\begin{aligned}
\overline{A_2}(R_0) &= \frac{1}{2}\frac{eqN^2\langle r^2\rangle_0}{R_0^3} \\
\overline{A_4}(R_0) &= \frac{1}{8}\frac{eqN^2\langle r^4\rangle_0}{R_0^5}.
\end{aligned} \tag{12}$$

Many studies have shown that $\overline{A_2}/\overline{A_4}$ is constant for $3d^n$ ions (Edgar 1976, Newman *et al* 1978, Yeung and Newman 1986), as can be expected from equation (12). Using these equations, it is calculated that $\overline{A_2}(R_0) = 5070\ cm^{-1}$ and $\overline{A_4}(R_0) = 672\ cm^{-1}$ for $N = 0.956$, and that $\overline{A_2}(R_0) = 4927\ cm^{-1}$ and $\overline{A_4}(R_0) = 656\ cm^{-1}$ for $N = 0.942$. The values of B_{kq} in equation (11) can be calculated by considering the parameters $\overline{A_2}$ and $\overline{A_4}$ as well as the arrangement of O^{2-} ions around Na^+ and N^{3+} sites (table 2), such as those in the PCM. The theoretical ZFS parameters D_{Na}^{SPM}, E_{Na}^{SPM}, D_N^{SPM} and E_N^{SPM} for the Mn^{2+} ion at both sites calculated with this model are summarized in table 4, together with the experimental values. As shown in this table, this model also gives the same results as the PCM; the order of magnitude of D_{exp} (E_{exp}) is more similar to that of D_{Na}^{SPM} (E_{Na}^{SPM}) than to that of D_N^{SPM} (E_N^{SPM}). This also implies that the Mn^{2+} ion should substitute for Na^+ rather than N^{3+}.

As shown in tables 3 and 4, both models reveal that the value of D_{Na}^{SPM} (E_{Na}^{SPM}) at $N = 0.942$ is closer to that of D_{exp} (E_{exp}) than at $N = 0.956$. Figure 1 shows the comparison of the theoretical ZFS parameters and the experimental data at several N-values including $N = 0.942$ and 0.956, where the theoretical values increased with decreasing N. As can be seen from this figure, the value of D_{Na} (E_{Na}) at $N \simeq 0.8$ is very similar to that of D_{exp} (E_{exp}). On considering the covalency ($N \simeq 0.25$ for NO_2^-) assuming the substitution of Mn^{2+} for the N^{3+} site, D_N (E_N) at $N \simeq 0.25$ is of the order of magnitude of $10^4\ cm^{-1}$ and is much more different from D_{exp} (E_{exp}) than (about $10^1\ cm^{-1}$) at $N = 0.942$ and

Table 4. Comparison of the ZFS parameters calculated by the superposition model for Mn^{2+} at Na^+ and N^{3+} ions in $NaNO_2$ with the experimental data.

ZFS parameters	Theoretical				Experimental (Jain *et al* 1978)
	Na site		N site		
	$N = 0.942$	$N = 0.956$	$N = 0.942$	$N = 0.956$	
D (10^{-4} cm^{-1})	172	160	43 188	40 278	464
E (10^{-4} cm^{-1})	−5	−4	133 514	124 317	−144
E/D	<0	<0	>0	>0	<0

0.956. This consideration indicates apparently that the Mn^{2+} ion substitutes not for the N^{3+} site but for Na^+.

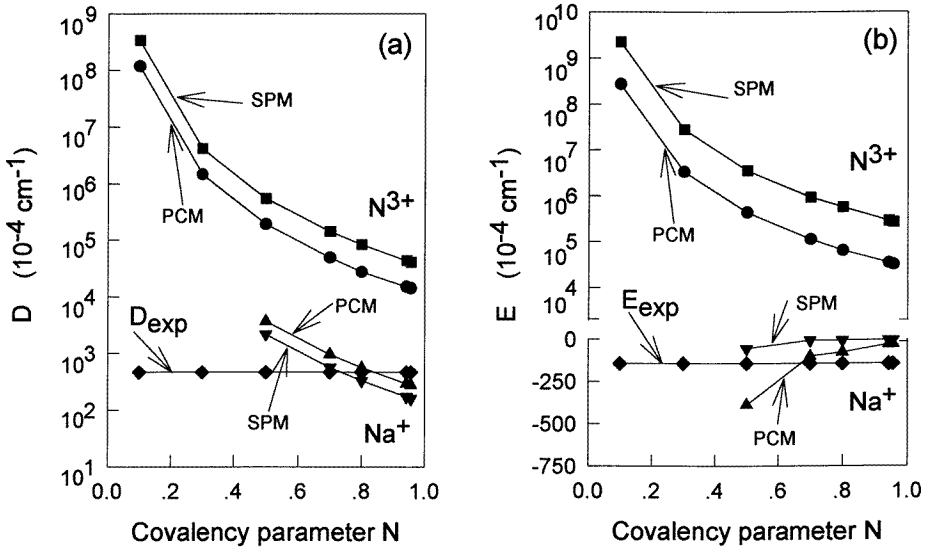

Figure 1. The ZFS parameters calculated as a function of the covalency parameter N: (a) D; (b) E.

Meanwhile, the values of D_{exp} at several temperatures have been reported whereas E_{exp} at RT was given only by Jain *et al* (1978). Moreover, only the structural data at 433 K are available, besides those at RT; the cell dimensions at 443 K are $a = 3.668$ Å, $b = 5.669$ Å and $c = 5.363$ Å, and the parameters t, w, u and v at 443 K are $t = 0.4615 \pm 0.0010$, $w = 0.0764 \pm 0.0007$, $u = -0.0418 \pm 0.0006$ and $v = 0.1943 \pm 0.0006$ (Komatsu *et al* 1988). Thus we can compare the theoretical and experimental D-values only at the two temperatures ($D_{exp} = 0.0388$ cm^{-1} at 443 K). In order to investigate the change in D_{Na} and D_N with temperature, the theoretical values at $N = 0.8$ are calculated using the PCM and SPM; at RT, $D_{Na}^{PCM} = 0.0571$ cm^{-1}, $D_{Na}^{SPM} = 0.0341$ cm^{-1}, $D_N^{PCM} = 2.740$ cm^{-1} and $D_N^{SPM} = 8.307$ cm^{-1} and, at 443 K, $D_{Na}^{PCM} = 0.0487$ cm^{-1}, $D_{Na}^{SPM} = 0.0308$ cm^{-1}, $D_N^{PCM} = 2.732$ cm^{-1} and $D_N^{SPM} = 8.300$ cm^{-1}. The relations between the D-values at the two temperatures are as follows; for the experimental values D_{exp}(RT) > D_{exp}(443 K) and,

for the theoretical values $D_{Na}^{PCM}(\mathrm{RT}) > D_{Na}^{PCM}(443\ \mathrm{K})$ and $D_{Na}^{SPM}(\mathrm{RT}) > D_{Na}^{SPM}(443\ \mathrm{K})$, but $D_{N}^{PCM}(\mathrm{RT}) \simeq D_{N}^{PCM}(443\ \mathrm{K})$ and $D_{N}^{SPM}(\mathrm{RT}) \simeq D_{N}^{SPM}(443\ \mathrm{K})$. This result can be understood by the fact that the molecular structure of NO_2^- is not changed irrespective of temperature, unlike the bond length of Na^+–O^{2-}. Thus, D_N is calculated to be almost constant in the whole temperature range of ferroelectric and paraelectric phases. However, the NO_2^- radical actually experiences torsional motions around the crystallographic axes. These motions become more activated with increasing temperature, resulting in a reduction in D_N. The reduction in D for both sites at higher temperatures can also be deduced from the temperature dependence data of the quadrupole coupling constants Q_{cc} for those nuclei (^{23}Na and ^{14}N) reported by many investigators (see e.g., Oja *et al* (1967) and Han and Choh (1993)) since D is closely related to Q_{cc} (Burns 1962, Stankowski 1969, Choh *et al* 1989). Q_{cc} for both ^{23}Na and ^{14}N was reported to decrease with increasing temperature, unlike the case of $LiNbO_3$:Mn^{2+} in which D and Q_{cc} for Li monotonically increased with increasing temperature and those at Nb decreased (Choh *et al* 1989, Jain 1992). Thus we cannot estimate the probable site of Mn^{2+} in $NaNO_2$ from the temperature dependence of D_{Na} and D_N since they have similar temperature dependences.

In addition to the analyses by the PCM and SPM, we compared the chemical properties for both sites such as the ionic radii and the bond lengths. The ionic radius of Mn^{2+}, $r(Mn^{2+}) = 0.8$ Å, is similar to that of Na^+, $r(Na^+) = 0.97$ Å, but is about five times that of N^{3+}, $r(N^{3+}) = 0.16$ Å. Moreover, the bond length (2.2 Å) of Mn^{2+}–O^{2-}, being the sum of $r(Mn^{2+})$ and $r(O^{2-})$, is far more comparable with that (2.47 Å) of Na^+–O^{2-} than with that (1.23 Å) of N^{3+}–O^{2-}. These facts also support the replacement of Na^+ by the Mn^{2+} ion. These considerations including the change in D with temperature are summarized in table 5 together with the PCM and SPM results, and all of them support the fact that the Mn^{2+} ion substitutes for the Na^+ ion.

Table 5. Several comparisons supporting the substitution of Mn^{2+} for the Na^+ site.

	Comparisons	Probable site (supported by the first column)
PCM/SPM	See tables 1 and 2	Na^+
Ionic radius	$r(Mn^{2+})/r(Na^+) = 1.2$, $r(Mn^{2+})/r(N^{3+}) = 5$	Na^+
Bond length	Na–O, 2.47 Å N–O, 1.23 Å $r(Mn^{2+}) + r(O^{2-}) = 2.2$ Å	Na^+
Covalency effect at $N \simeq 0.25$ for NO_2^-	D_N (E_N) at about 0.25 are quite different from D_{exp} (E_{exp}) compared with the situation at $N = 0.942$ and 0.956 (see figure 1)	Na^+
Temperature dependence of D	Theoretical $D_{Na}^{PCM}(\mathrm{RT}) > D_{Na}^{PCM}(443\ \mathrm{K})$ $D_{Na}^{SPM}(\mathrm{RT}) > D_{Na}^{SPM}(443\ \mathrm{K})$ $D_{N}^{PCM}(\mathrm{RT}) \simeq D_{N}^{PCM}(443\ \mathrm{K})$ $D_{N}^{SPM}(\mathrm{RT}) \simeq D_{N}^{SPM}(443\ \mathrm{K})$ Experimental $D_{exp}(\mathrm{RT}) > D_{exp}(443\ \mathrm{K})$	—

In summary, the preferred site of the Mn^{2+} ion in $NaNO_2$ was first determined using the PCM and the SPM. As can be seen from tables 3 and 4, these models yield the same result that the experimental values are in reasonable agreement with the calculations considering Mn^{2+} at Na^+ sites and not at all of the order of magnitude of those obtained on the assumption that it substitutes for N^{3+} sites. Moreover, the signs of D_{exp} and E_{exp} are consistent with those of D_{Na} and E_{Na}: $D_{Na} > 0$, $E_{Na} < 0$ and $E_{Na}/D_{Na} < 0$. These results can be understood by the fact that the O^{2-} arrangement around Na^+ is suitable for theoretical values similar to the experimental data. From these results, one can conclude that the Mn^{2+} ion replaces the Na^+ site. This conclusion is also supported by comparisons of the chemical properties such as the ionic radii and the bond lengths and by consideration of the covalency of the NO_2^- radical.

References

Ambroseti R, Angelone R, Colligiani A and Rigamonti A 1977 *Phys. Rev.* B **15** 4318
Burns G 1962 *Phys. Rev.* **123** 1634
Curie D, Barthou C and Canny B 1974 *J. Chem. Phys.* **61** 3048
Choh S H, Kim H T, Choh H K, Han C S, Choi D and Kim J N 1989 *Bull. Magn. Reson.* **11** 3171
Edgar A 1976 *J. Phys. C: Solid State Phys.* **9** 4303
Han K T and Choh S H 1992 *J. Korean Phys. Soc.* **24** 159
——1993 *Solid State Commun.* **87** 119
Han K T, Yeom T H and Choh S H 1990 *Ferroelectrics* **107** 349
Jain V K 1992 *Solid State Commun.* **84** 669
Jain A K and Upreti G C 1978 *Chem. Phys. Lett.* **55** 506
Jain A K, Upreti G C and Srivastava K N 1978 *Phys. Lett.* **69** 50
Kanashiro T, Ohno T and Satoh M 1985 *J. Phys. Soc. Japan* **54** 2720
Kay M I 1972 *Ferroelectrics* **4** 235
Kay M I and Frazer B C 1961 *Acta Crystallogr.* **14** 56
Komatsu K, Itoh K and Nakamura E 1988 *J. Phys. Soc. Japan* **57** 2836
Luz Z, Reubeni A, Holmberg R W and Silver B L 1969 *J. Chem. Phys.* **51** 4017
Newman D J, Pryce D C and Runeiman W A 1978 *Am. Mineral.* **63** 1278
Nomura S 1961 *J. Phys. Soc. Japan* **16** 2440
Oja T, Marino R A and Bray P J 1967 *Phys. Lett.* **26A** 11
Serishev S A, Vinogrdova I S and Buznik V M 1974 *Sov. Phys.–Solid State* **16** 565
Sharma R R 1967 *Phys. Rev.* **171** 378
——1968 *Phys. Rev.* **176** 467
Sharma R R, Obarch R and Das T P 1966 *Phys. Rev.* **149** 257
Shen G Y and Zhao M G 1984 *Phys. Rev.* B **30** 3619
Stankowski J 1969 *Phys. Status Solidi* **34** K137
Takeno J and Gesi K 1964 *J. Chem. Phys.* **40** 1317
Yagi T and Tasuzaki I 1973 *J. Phys. Soc. Japan* **35** 1675
Yeom T H, Choh S H and Du M L 1993 *J. Phys.: Condens. Matter* **5** 2017
Yeom T H, Choh S H, Du M L and Jang M S 1996 *Phys. Rev.* B **53** 1
Yeung Y Y and Newman D J 1986 *Phys. Rev.* B **34** 2258
Yu W L 1990 *Phys. Rev.* B **41** 9215
Yu W L and Zhao M G 1987 *J. Phys. C: Solid State Phys.* **20** 4647
——1988 *Phys. Rev.* B **37** 9254
Zhao M G and Zhang Y F 1983 *IEEE Trans. Magn.* **MAG-19** 1972
Zhao M G, Du M L and Shen G Y 1987 *J. Phys. C: Solid State Phys.* **20** 5557